ARMY RESEARCH LABORATORY

1 MA Breech Upgrade for the U.S. Army Research Laboratory's (ARL's) Rectangular 22- × 44-mm In-bore Cross Section Railgun

by Miguel A. Del Güercio and Alexander Michlin

ARL-TR-5619 **August 2011**

NOTICES

Disclaimers

The findings in this report are not to be construed as an official Department of the Army position unless so designated by other authorized documents.

Citation of manufacturer's or trade names does not constitute an official endorsement or approval of the use thereof.

Destroy this report when it is no longer needed. Do not return it to the originator.

Army Research Laboratory
Aberdeen Proving Ground, MD 21005

ARL-TR-5619 **August 2011**

1 MA Breech Upgrade for the U.S. Army Research Laboratory's (ARL's) Rectangular 22- × 44-mm In-bore Cross Section Railgun

Miguel A. Del Güercio and Alexander Michlin
Weapons and Materials Research Directorate, ARL

REPORT DOCUMENTATION PAGE

Form Approved
OMB No. 0704-0188

1. REPORT DATE *(DD-MM-YYYY)*	2. REPORT TYPE	3. DATES COVERED (From - To)
August 2011	Final	July 2009 to January 2010

4. TITLE AND SUBTITLE
1 MA Breech Upgrade for the U.S. Army Research Laboratory's (ARL's) Rectangular 22- × 44-mm In-bore Cross Section Railgun

5a. CONTRACT NUMBER

5b. GRANT NUMBER

5c. PROGRAM ELEMENT NUMBER

6. AUTHOR(S)
Miguel A. Del Güercio and Alexander Michlin

5d. PROJECT NUMBER

5e. TASK NUMBER

5f. WORK UNIT NUMBER

7. PERFORMING ORGANIZATION NAME(S) AND ADDRESS(ES)
U.S. Army Research Laboratory
ATTN: RDRL-WML-D
Aberdeen Proving Ground, MD 21005

8. PERFORMING ORGANIZATION REPORT NUMBER
ARL-TR-5619

9. SPONSORING/MONITORING AGENCY NAME(S) AND ADDRESS(ES)

10. SPONSOR/MONITOR'S ACRONYM(S)

11. SPONSOR/MONITOR'S REPORT NUMBER(S)

12. DISTRIBUTION/AVAILABILITY STATEMENT
Approved for public release; distribution is unlimited.

13. SUPPLEMENTARY NOTES

14. ABSTRACT
The 4.5-MJ capacitor-based power supply at the U.S. Army Research Laboratory (ARL) originally contained 18 modules at 250 KJ each. Within each module, five 840-μF Aerovox capacitors and either a 60-μH or a 30-μH inductor, allowed the generation of output pulses of different profiles. Since 2001, the power supply, railgun and breech, has performed safely and reliably for over 500 single–shot launches. During 2007, all capacitors were replaced with new 950-μF General Atomics capacitors, increasing the total energy of the system to 5.2 MJ. During 2009 a study was started to assess the feasibility of modifying the existing breech that would result in a breech of smaller size, improved means to load projectiles, and capable of firing multiple shots at 1 MA. A first analysis focused on improving the uniformity of current distributions at the breech-insert-rail interfaces, suspected in causing of some catastrophic failures seen previously during multi-shot launches. Next, the breech contact forces were characterized as well as selection of improved materials and geometries for the breech plates and rail inserts. This report includes progress made until the facility was shutdown in November 2009 and contains general conclusions to facilitate the implementation of a multi-shot 1-MA breech.

15. SUBJECT TERMS
1 MA breech, railgun

16. SECURITY CLASSIFICATION OF:			17. LIMITATION OF ABSTRACT	18. NUMBER OF PAGES	19a. NAME OF RESPONSIBLE PERSON
a. REPORT	b. ABSTRACT	c. THIS PAGE	UU	32	Miguel A. Del Güercio
Unclassified	Unclassified	Unclassified			19b. TELEPHONE NUMBER (*Include area code*) (410) 278-3773

Contents

List of Figures

List of Tables

Acknowledgments

The authors wish to thank Mr. Robert Glassman (Dynamic Science, Inc) and Mr. Anthony Canami, whose assistance in testing with shorted discharges at the breech is greatly appreciated. The authors also wish a special thanks to Dr. Charles Hummer (Physics Phenomenology Branch) and Mr. Peter Denny, a Johns Hopkins summer student for their technical contributions to this report.

1. Introduction

During 2001, a 4.5-MJ capacitor-based system,[1] a charging DC power supply, a 3.1-m-long, 22- × 44-mm in-bore cross-section railgun and breech (figure 1a) were commissioned at the U.S. Army Research Laboratory (ARL) as an operational railgun system. During 2007, this 840-μF Aerovox capacitor-based system from Physics International was updated with General Atomics state of the art 950-μF capacitors, increasing the total breech energy to 5.2 MJ. The extensive use of the breech and railgun had shown the need to implement a better breech-insert-rail interface, and a simpler breech-railgun coupling to facilitate armature loading. It has been ARL's experience, especially during multi-shot testing, to avoid disrupting the breech-insert-rail interfaces, i.e., replacing inserts, or changing the breech bolts torque (figure 1a), as catastrophic arcs between the breech plates and rails interfaces could occur with greater frequency when these actions take place. Armature loading during single and multi-shot launches is a laborious and time consuming process, requiring the removal of the first and second railgun containments (figure 1b). Accordingly, desirable new features would include: (1) breech design that minimizes localized high current density areas at the breech-rails interface, (2) multi-shot capability at 1MA, (3) armature loading without removing railgun containments, and (4) compact breech design that will reduce the bulk size of the present coaxial connections.

To keep the breech-insert-rail interfaces intact at higher energy and peak currents, higher contact forces were implemented to help eliminate arcing at the areas of localized high current density (figure 1c). One of the first areas of study has been on the affects of breech plate geometry on the uniformity of current distribution at the breech-rail interface, since the present design exhibits a significant non-uniform current distribution.

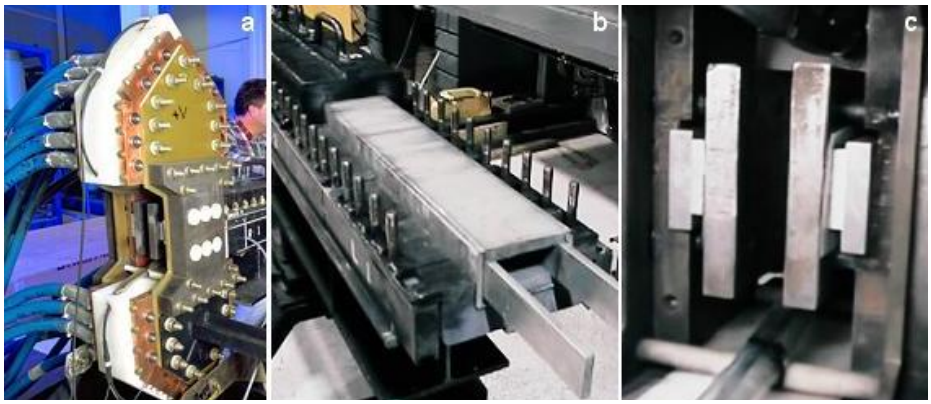

Figure 1. Present Breech (1a), exposed first section of railgun (1b), breech plates, and breech-rail interface detail (1c).

[1] Del Güercio, M. *ARL Commissioning Experiments With a 4.5-MJ Pulsed Power Supply*; ARL-TR-2814; U.S. Army Research Laboratory: Aberdeen Proving Ground, MD, 2002.

In the current design, extensive damage to the rails (6262-T6 aluminum) and copper inserts is always observed on a rail area with a higher current densit, or in the area of the leading edge closest to the first railgun containment (figure 2a). Rail sections positioned furthest into the breech exhibit a lower current density and reduced damage. Damage to the steel breech clamping plates, due to arcing at the copper inserts, can also be extensive. Damage is also evident at lower currents as can be seen in the photo and laser scan of the breech end of the rails (figure 2b).

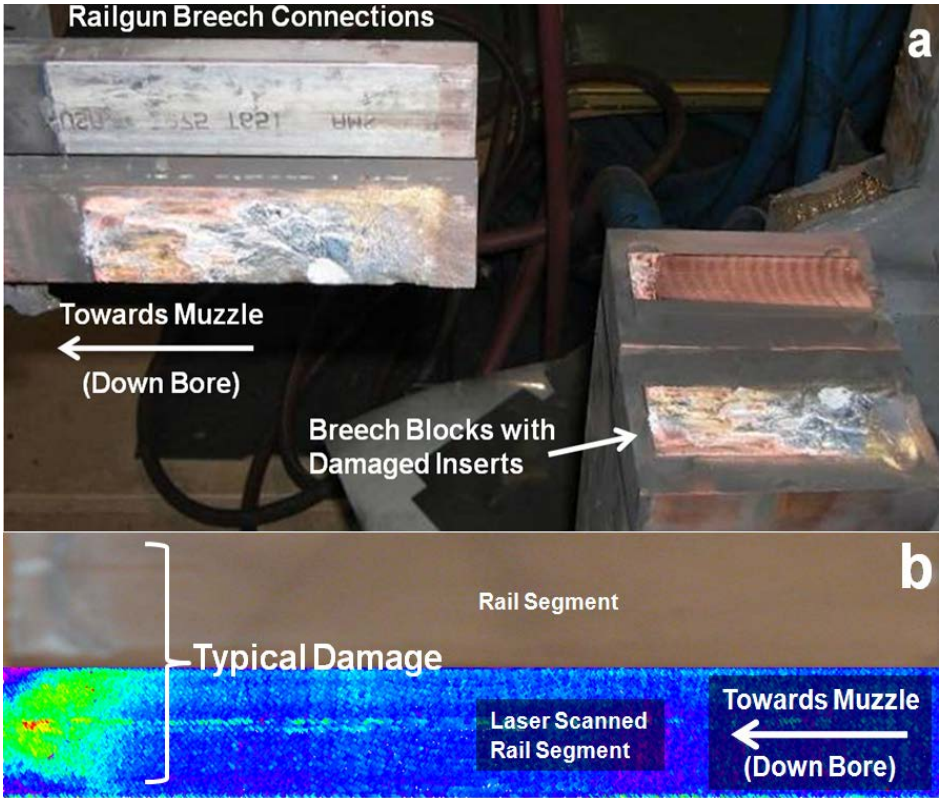

Figure 2. Undesired effect of non uniform current density on rail-insert interface, (images are not to scale).

2. Improved Uniform Current Distribution Through Breech Geometry

To investigate a breech geometry that would contribute to improving the uniformity of the current distribution at the rail-insert interface, a rectangular plate was cut from a stock 0.25-in-thick aluminum plate. Homemade magnetic field sensors (so-called B-dots) were positioned on a linear array (figure 3) to map the current distribution across the aluminum plate. Twelve B-dot magnetic field sensors captured the magnetic fields generated by the current in the plate. The resultant signals from the sensors were recorded with a transient data recorder.

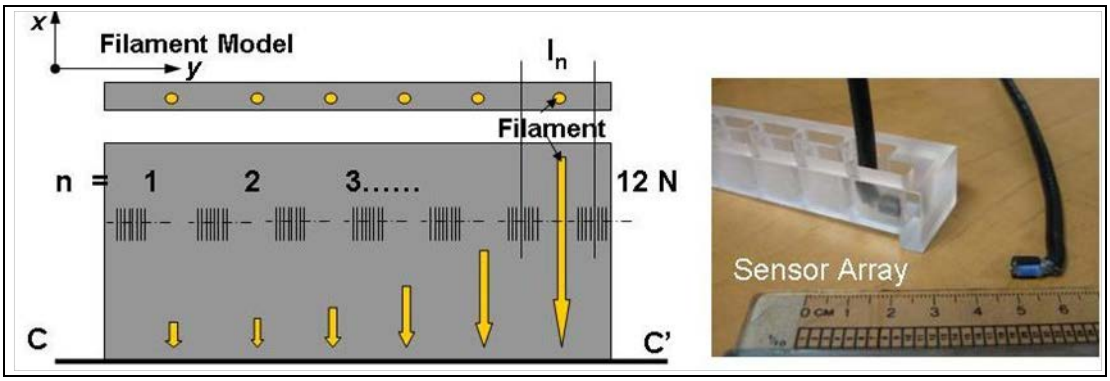

Figure 3. B-dots array and single B-dot inside the 12-sensor acrylic holder, one current filament is considered per B-dot.

To measure the current distribution from magnetic field of an arbitrary shaped conductor, which can be a daunting task, a single cylindrical current-carrying conductor, such as a wire, was considered. The magnetic field B generated around a cylindrical conductor of radius, r, decreases inversely with the radius, and can be expressed as:

$$B = \mu_0 I / 2\pi r \quad (1)$$

where

B = magnetic field

μ_0 = permeability of free space ($1.25663706 \times 10^{-6}$ m kg s^{-2} A^{-2})

I = current (amps)

r = radius from the conductor (m)

The magnetic field can also be calculated from experimental measurements by integrating the measured voltage of a B-dot at the particular position as in equation 2. In order to simply the calculations and measurements, a plate conductor can be thought of as multiple “wires”, or “n” number of filaments.

$$By_n = K \int v_0 \, dt \quad (2)$$

where

K = calibration constant

v_0 = voltage measured by the probe

The current of each filament, I, is then calculated from the magnetic field using

$$I_x = 2\pi \, r \, B_y / \mu_0 \tag{3}$$

$$I = \sum_{i=1}^{n} 2\pi \, r \, B_i / \mu_0 \quad \text{or} \quad I = 2\pi \, r \, B_{1\ldots12} / \mu_0 \tag{4}$$

$$I = \sum_{i=1}^{12} \frac{1}{\mu_0} 2\pi r (K \int V_0 dt) \tag{5}$$

The variable "r" is considered the same for each sensor due to the geometry and defined as the radius of an ideal current filament to the B-dot. With 12 B-dot measurements, the plate was simplified to 12 ideal current filaments. The current in each filament can be calculated using equation 3; however, the value for "r" is not yet precisely known. The total current through the plate can be thought of as the summation of the 12 ideal current filaments equation 4. When equation 2 is combined with equation 4 and set equal to the total measured current equation 5, a combined value for "r*K" can be found.

Once an initial value of "r*K" is found and the individual filament currents calculated for a specific time, the process for finding "r*K" was repeated at different time steps (0.5 ms, 1 ms, 2 ms, and 3 ms). By iterating the value of "r*K" over the different time steps, a good overall match of the measured currents can be reached as seen in the top right of figure 4.

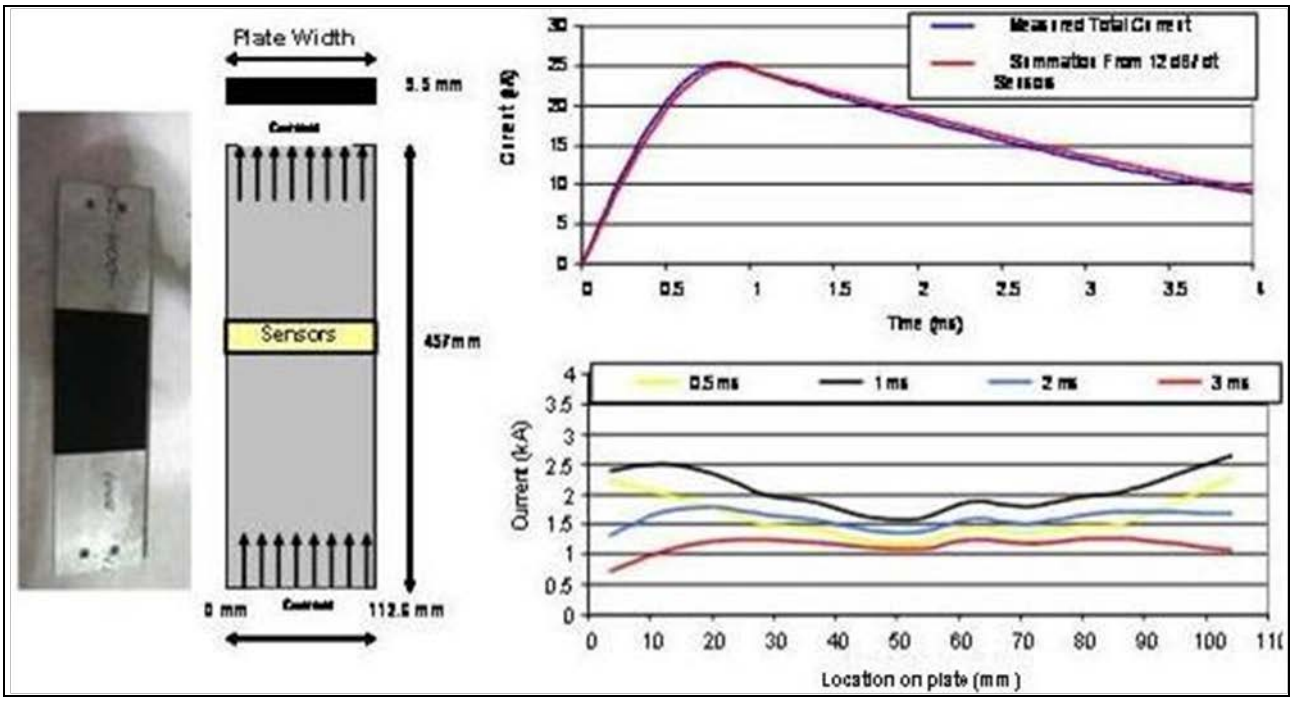

Figure 4. Straight plate, sensor array location, integrated and measured current data from output pulse and current filaments across section of straight plate.

A theoretical current distribution, provided by Charles Hummer, PPB, simulating the conditions in the test is shown in figure 5a. The theoretical current distribution used 16 filaments instead of

12 to provide a more detail. The calculated current distribution from the B-dots show acceptable agreement with the theoretical predictions for a plate modeled as a set of wires for 2 ms and 3 ms as can be seen in figure 5b. Lower than expected measurements at the plate edges were expected due to the coarseness of the B-dot sensor array. The summation of individual B-dot current measurements agreed with the total current measurement taken on the existing breech, which can be seen in figure 5c. This agreement lends confidence to the validity of the individual B-dot measurements performed.

The most deviation occurs closest to the plate edges at the earliest times due to the higher current density caused by “skin” effects, when the current has not diffused throughout the thickness of the plate.

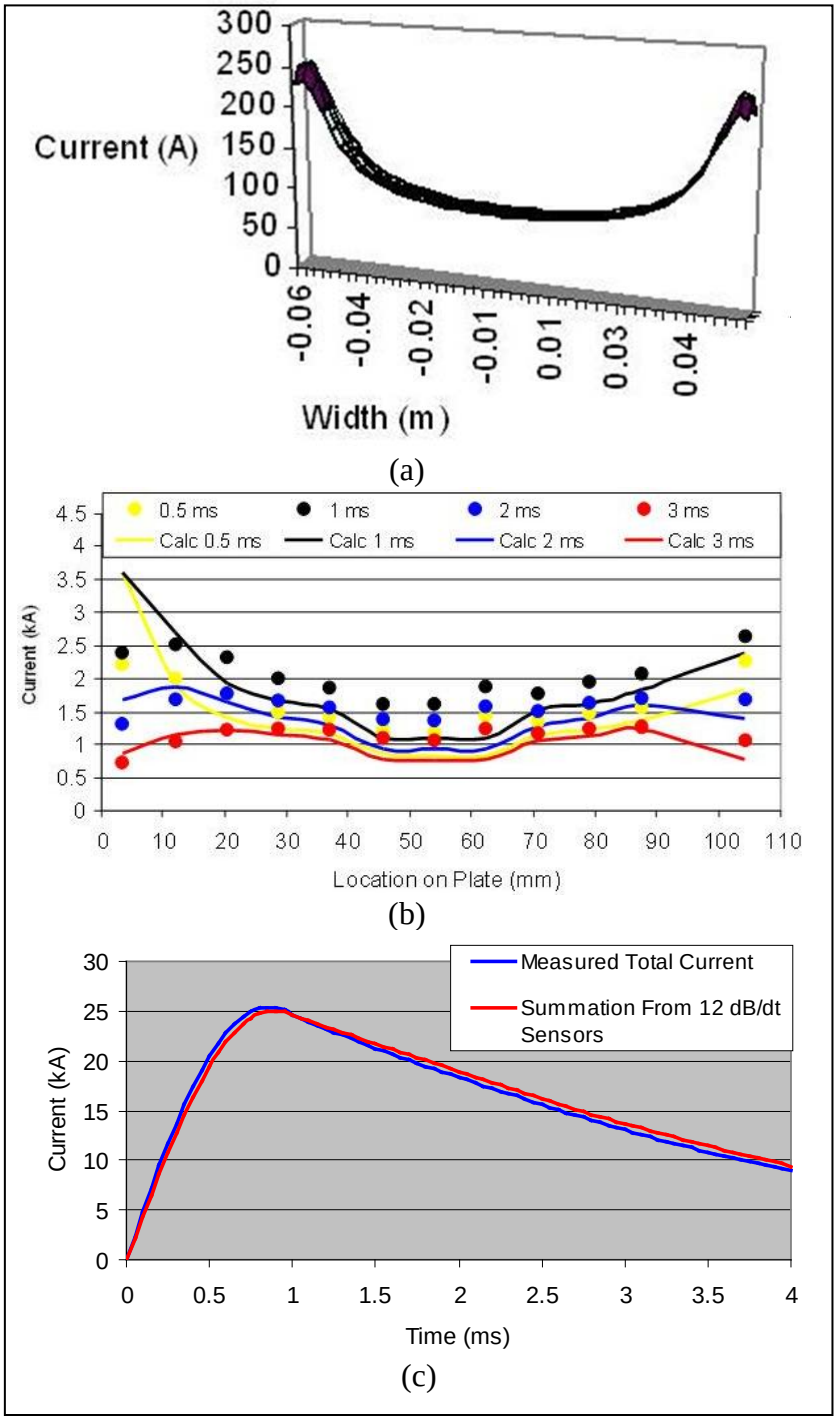

Figure 5. (a) Theoretical calculation by Dr. Charles Hummer of 4 × 4, 16 filaments B-dot at 1 ms, (b) current profiles of calculations versus data of a section of the straight plate, (c) B-dot summation current plotted with total breech current.

Having determined that the measured data for the straight plate was in agreement with the theoretical calculations, the sensor array was attached to a 0.25-in-thick aluminum surrogate plate (figure 6) resembling half of the existing copper breech coaxial termination points (labeled 1, 2, 3, and 4 on figure 6). The sketch represents one copper breech element with a right angle extension simulating a single rail of the railgun.

Since the existing breech has 18 independently-triggered capacitor bank connections spread along the coaxial termination points; different current pulse shapes can cause current to flow into some termination points and not others at any given point in time. To account for the different pulse shape current paths, three test configurations were tested:

- Four connections at the front: two connections at location 1, two connections at location 2.
- Four connections at the rear: two connections at location 3, two connections at location 4.
- Symmetric, normal operation: one connection at 1, 2, 3, and 4.

The trapezoidal section of the plate was connected utilizing the above connections to the breech return path (negative), while the positive end labeled railgun (figure 6), was connected to the (positive) breech output, closing the test circuit. The B-dot sensor array axis was positioned along the E-C orientation.

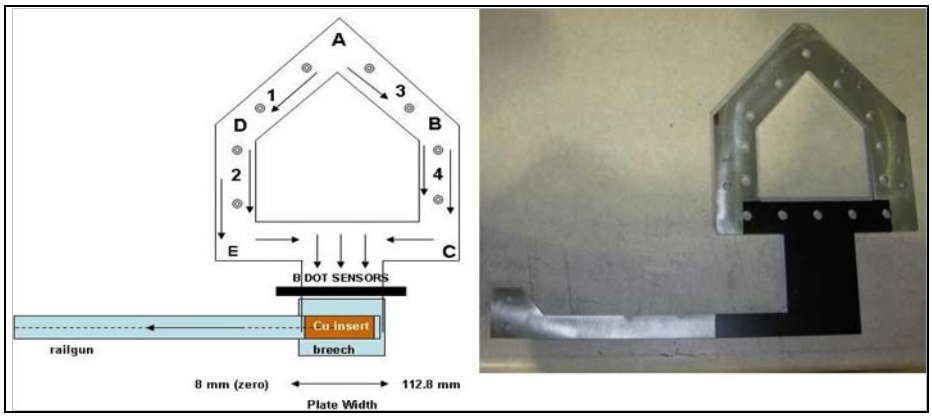

Figure 6. Sketch and photo of mockup of one of the four breech copper elements.

The highest current densities are observed closest to the “zero” end of the plate located closest to the railgun containments. In turn, the lowest current density in the insert area appeared furthest from the railgun containments. The trend in current density distribution remained largely unaffected by changing the attachment points for the current flow measurements. The percent current distribution versus plate location is plotted in figure 7, where the “zero” location represents the edge of the plate closest to the railgun containments. From the graph, one can see that one-third of the total current passes through in the first 12 mm (approximately 0.5 in or one-tenth) of the plate width as shown in figure 8. The location of the highest current densities also agrees with damage observed visually and from laser scans of the rails.

Figure 7. "B-dots" plate current measurement integrated over 1 ms versus plate position.

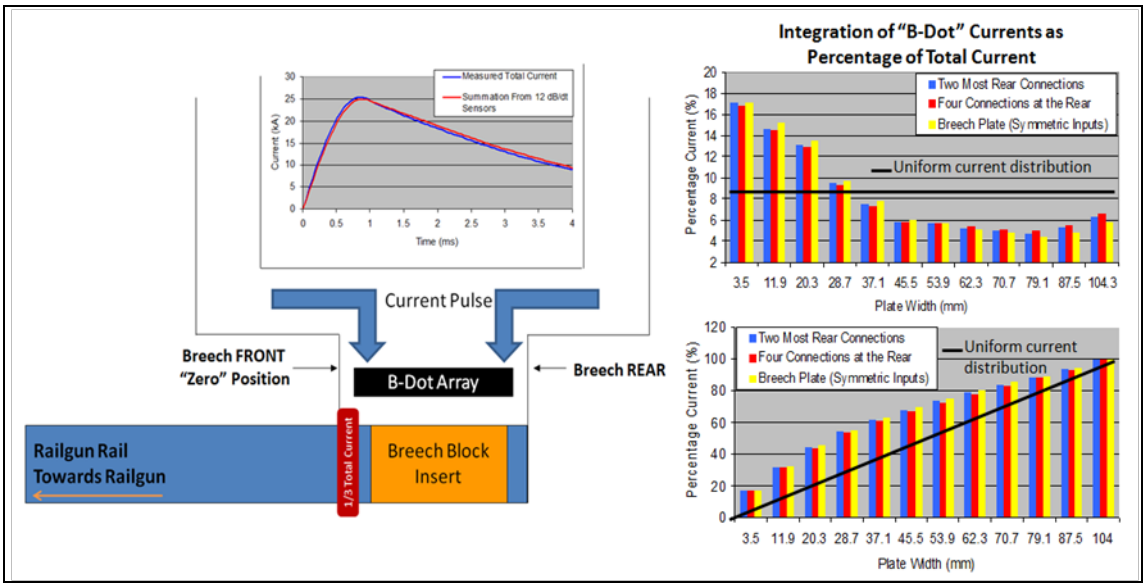

Figure 8. One-third of the total breech c urrent appears in the first one-tenth of electrical rail contact.

Attempting to more evenly distribute the current density, several slots were cut into the surrogate plate: straight slot, closed "L" slot, and a "thru L" slot as seen in figure 9, and tested in a similar manor as before.

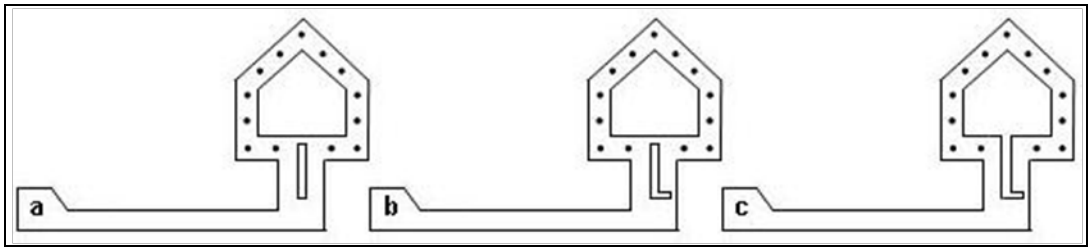

Figure 9. Surrogate plate with closed slot cavity (a), closed "L" shaped slot (b), and "thru L" shaped slot (c).

Plotting the cumulative percentage current versus location on the surrogate plate with a closed straight slot (figure 10) and a closed "L" slot (figure 11) reveals a similar cumulative percentage current distribution from the unmodified surrogate plate as shown in figure 8. The "thru L" slot, seems to have modified the current density slightly as shown in figures 12 and 13 when compared to the unmodified surrogate plate.

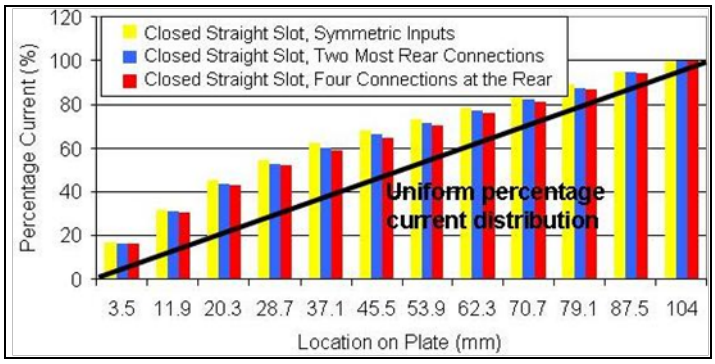

Figure 10. Cumulative measured percent current distribution for a surrogate plate with a closed straight slot.

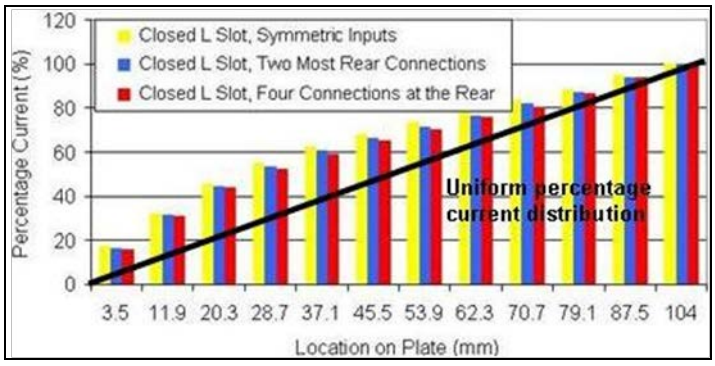

Figure 11. Cumulative measured percent current distribution for a surrogate plate with a closed "L" slot.

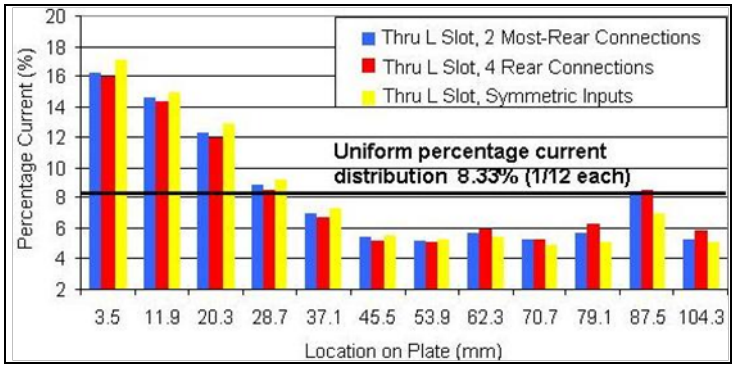

Figure 12. Local values of B-dot currents as percentage of total current ("thru L" slot), figure 9c, showing slight improvement over the unmodified plate.

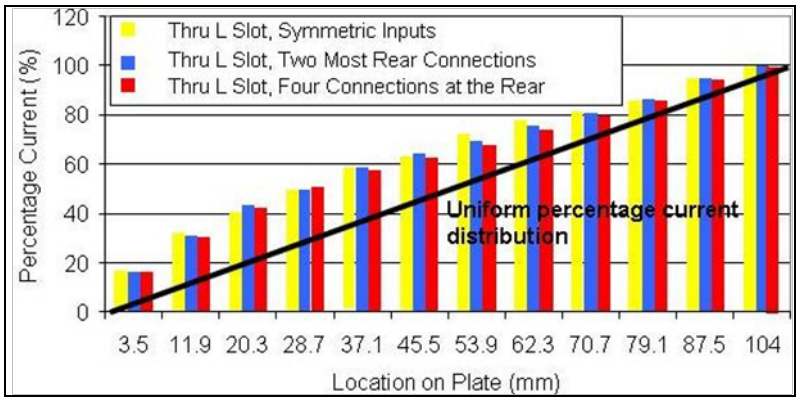

Figure 13. Cumulative percentage current distribution for a surrogate plate with a "thru L" slot.

Next, an open straight (figure 14a) was added to the area of highest current density to further the force current density away from the highest density region. The combined open straight slot and "thru L" slot improved the current distribution at the leading edge of the breech plate. The measured currents from the B-dot as percentage of total current is shown on figure 15, and the percentage of total currents versus surrogate plate location on figure 16.

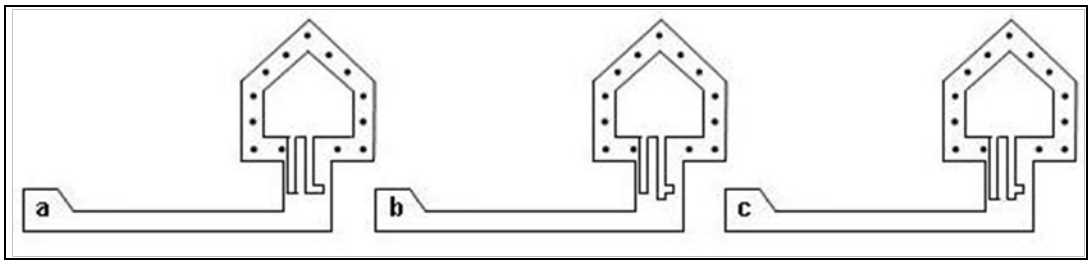

Figure 14. Different combinations of open cavity shapes: open straight and "L" slots (a), open straight and extended "L" slots (b), open straight and extended "L" slots (c).

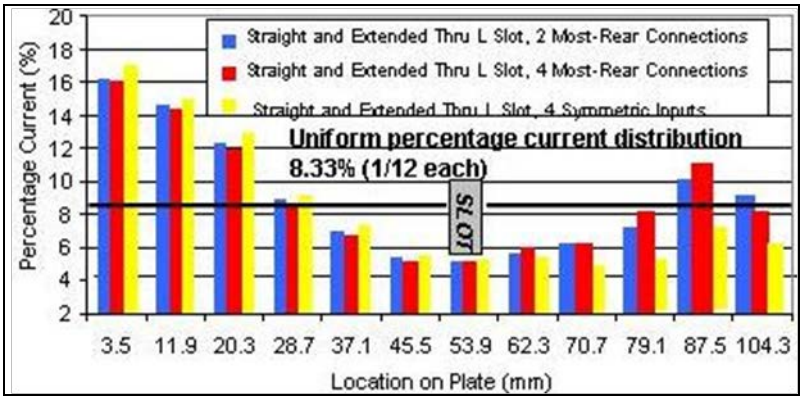

Figure 15. Local values of B-dot currents versus plate width for the open straight and "thru L" slots, showing more even current distribution at the ends.

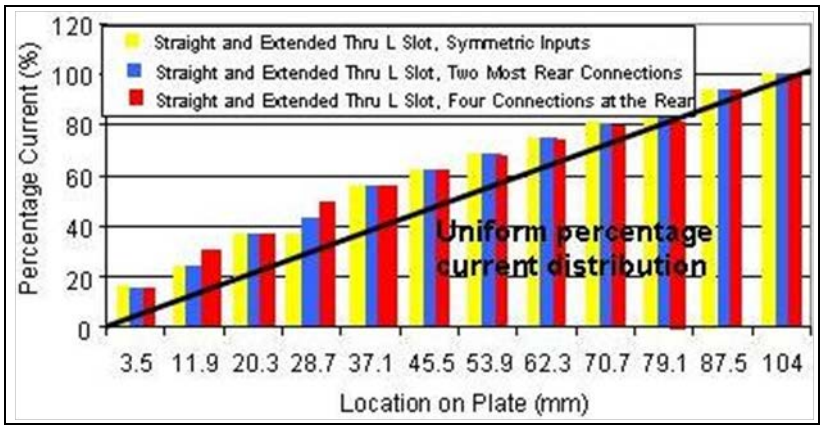

Figure 16. Cumulative percentage current distribution for a surrogate plate with open straight and "thru L" slot.

This geometry had increased the current density towards the back side of the breech plate in the 80-mm to 100-mm region and diverted current away from the densest area. Final analysis was not finished for the surrogate plate configurations shown in figures 14b and 14c. The preliminary results indicate that a new breech plate configuration could be configured with slots to improve the current distribution. This improvement would diminish damage resulting from the application of higher current loading to the rail-insert interface that has been seen with the current breech plate design.

3. Effects of Multiple Discharges Into a Shorted Breech

One way to discharge energy through the breech repeatedly without launching an armature is by the use of a "U"-shaped short secured to the breech. Due to the forces generated by the existing "U" short, we established that the discharge currents should not exceed approximately 600 KA when utilizing this short. The permanent deformation of the "U" short in figure 17 occurred during a 620 KA pulse compared with a new "U" short. To contain the lateral forces during testing, the "U" short was supported by a through-bolted, two-piece black nylon clamp structure as seen in figure 18a. The clamp was designed to operate at currents up to 600 KA peak.

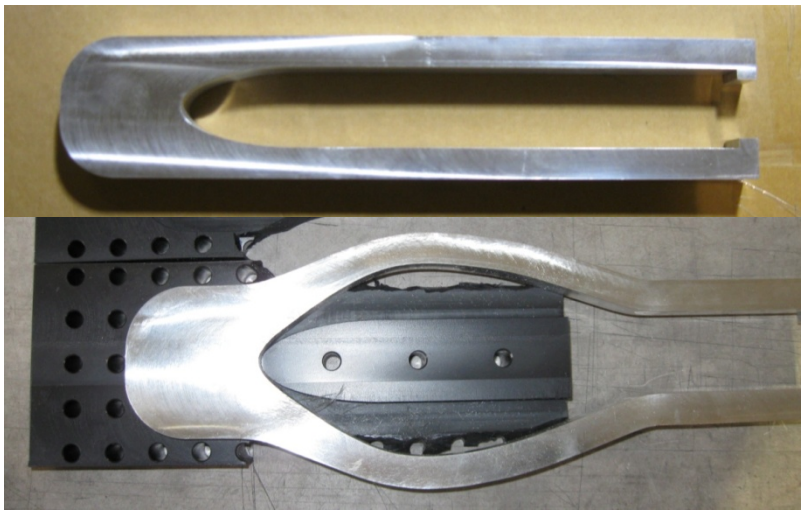

Figure 17. Typical "U" short at top and deformed "U" short due to the EM forces at bottom.

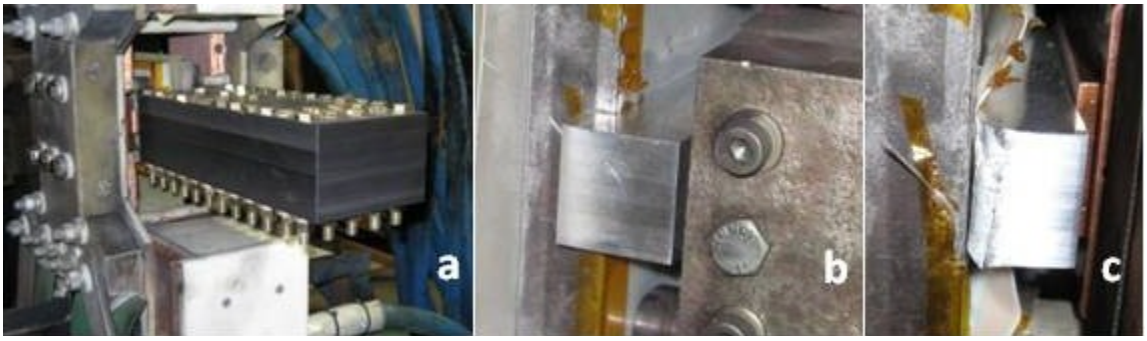

Figure 18. (a) Pre-test "U" short assembly showing black nylon clamp structure, (b) locked "U" short feet before, and (c) severed after discharge.

Table 1 includes the results of a simulated pulse utilizing Spice code (Intusoft Software, San Pedro CA) for "U" short testing up to 1MA peak current.[2] The firing times of the first ten modules were staggered at 20 µs from each other, while the times for the 11th and 12th modules were 300 µs, the firing time for modules 13th, 14th, and 15th was 600 µs each. Timing for modules 16th, 17th, and 18th times were 960 µs, 1080 µs, and 1240 µs respectively. This arrangement produced a flat pulse with fast rise time and smooth decay. A summary of the test results can be seen in table 2. The black nylon clamp held the "U" short successfully at just over 600 KA peak current with no failure cracks detected. During the third test, however, the "U" short failed with the locking feet sheared off, due to the electromagnetic forces trying to launch the short (figures 18b and 18c).

[2] *Del Güercio, M. A Spice-based Code for ARL's 4.5-MJ Electromagnetic Launcher Pulsed Power Supply System*; ARL-TR-2592; U.S. Army Research Laboratory: Aberdeen Proving Ground, MD, 2001.

Table 1. Simulated parameters for testing the "U" short to catastrophic failure.

Spice Simulation of Selected Pulse				
Charge Voltage	**Peak current**	**J(KA/mm)**	**Power MGW**	**Energy (KJ)**
4.0 KV	500 KA	19	76	129
5.0 KV	620 KA	24	117	200
6.0 KV	741 KA	29	169	288
7.0 KV	865 KA	34	229	392
8.0 KV	980 KA	39	300	510
8.25 KV	1.0 MA	40	317	542

Table 2. Summary of "U" testing with hardware failures noted.

Test/Pulse Number	Charge (KV)	Measured Current (KA)	U-Short Integrity	Comments
1	4.0	488 peak	OK	First pulse in first series
2	5.0	614 peak	OK	
3	6.0	740 peak	failed	fractured retaining feet
4	4.0	487 peak	OK	First pulse in 2nd series
5	5.0	611 peak	OK	
6	6.0	738 peak	OK	
7	6.5	737 peak	questionable	low current – possible unseen damage to short
8	6.5	783 peak	failed	containment and "U"-short failure
9	5.0	620 peak	OK	First pulse in third series
10	5.0	617 peak	OK	
11	5.0	613 peak	OK	
12	5.0	613 peak	OK	
13	5.0	611 peak	OK	
14	5.0	620 peak	failed	containment and "U"-short failure
15	5.0	618 peak	OK	First pulse in fourth series
16	5.0	621 peak	OK	
17	5.0	619 peak	failed	containment and "U"-short failure

Testing continued after adding brackets (figure 19) to restrain the launch forces on the "U" short. The subsequent tests performed as expected until test 7, which had a lower than expected current. Test 8, which was a repeat of test 7, gave an expected peak current of 783 KA, however the "U" structure and the short failed catastrophically with extensive damage to the breech coaxial cables and other adjacent components.

Figure 19. Pre-test assembly secured with extra brackets, and post-test failure from test 8 783 KA.

Having determined that the “U” short fractured at a current of 775 KA, the current was lowered to approx 80%, or around 620 KA (figure 20), to keep the “U” short intact for repetitive discharges.

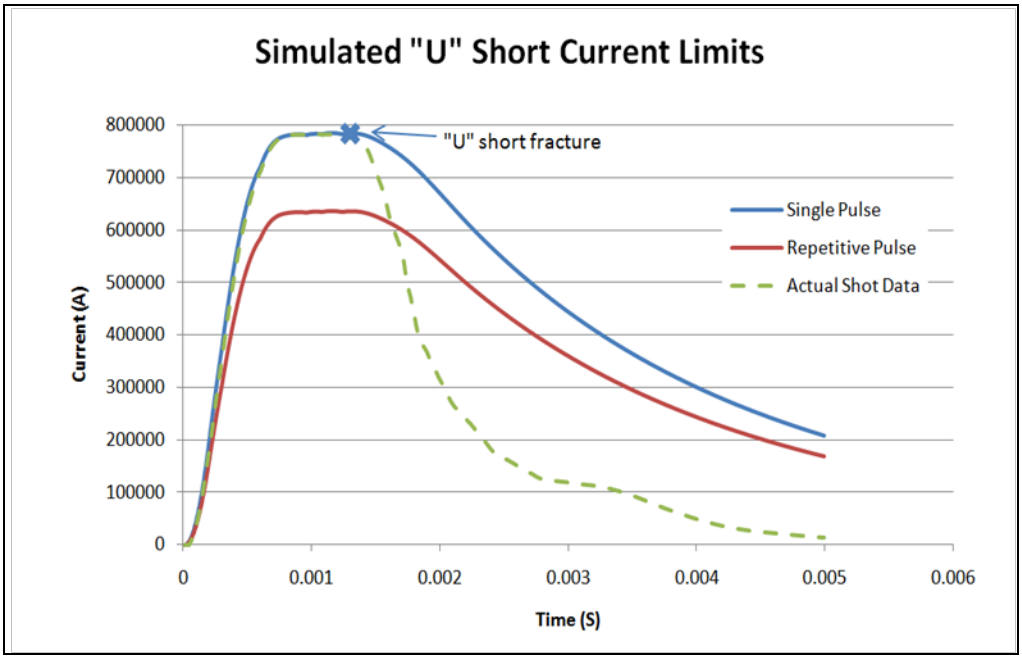

Figure 20. Current pulses used to test “U” short and inserts.

A test series with five and ten pulses was planned at a 620 KA current level. Kevlar cloth was wrapped around the “U” short containment (figure 21) before starting the series to help protect other components from damage if further “U” short failures occurred. The first five pulse series performed without any problems, and the copper inserts were evaluated afterwards.

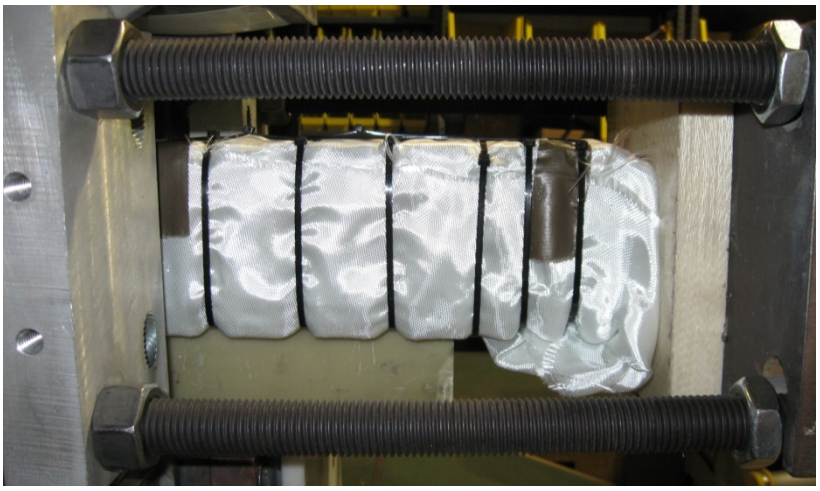

Figure 21. Kevlar cloth was wrapped around the nylon clamps containing the “U” short.

Another series of ten consecutive discharges into the shorted breech followed, so a new “U” short was installed in the same method as used in the previous consecutive series. The first discharge into the “U” short caused the short to deform and fractured the containment even though the same charge voltage and peak current had been used successfully in test 14. The failure was assumed to be caused by the short being made from a different grade of aluminum or unseen damage to the containment structure. The aftermath can be seen from figures 22 and 23.

Figure 22. Kevlar wrapping destroyed by fragmentation of retaining bracket.

Figure 23. Post-test nylon bracket condition.

After replacing the “U” short, testing was resumed, but the “U” short failed on the third repetitive discharge (test 17). None of the copper inserts from the test series showed the expected damage, which is likely due to realization of lower than desired current levels. Because of the unexplained structural failures of the “U” short, progress could not be made on testing at higher currents. The planned study to produce a design that would allow the loading of armatures without disconnecting the rails from the breech or opening any of the railgun containments was ended prematurely due to the railgun facility shut down on November 2009 for other programmatic reasons.

4. Measurement of Contact Forces at the Breech

Testing of the breech continued with non-energized measurements. Load cells were positioned longitudinally along the breech insert between the insert and the breech block to measure the contact forces as shown in figure 24. The contact area closest to the railgun was expected to experience a lower force than the opposite end, the area towards the rear end of the breech due to the non-symmetrical position of the breech blocks with respect to the clamping bolts.

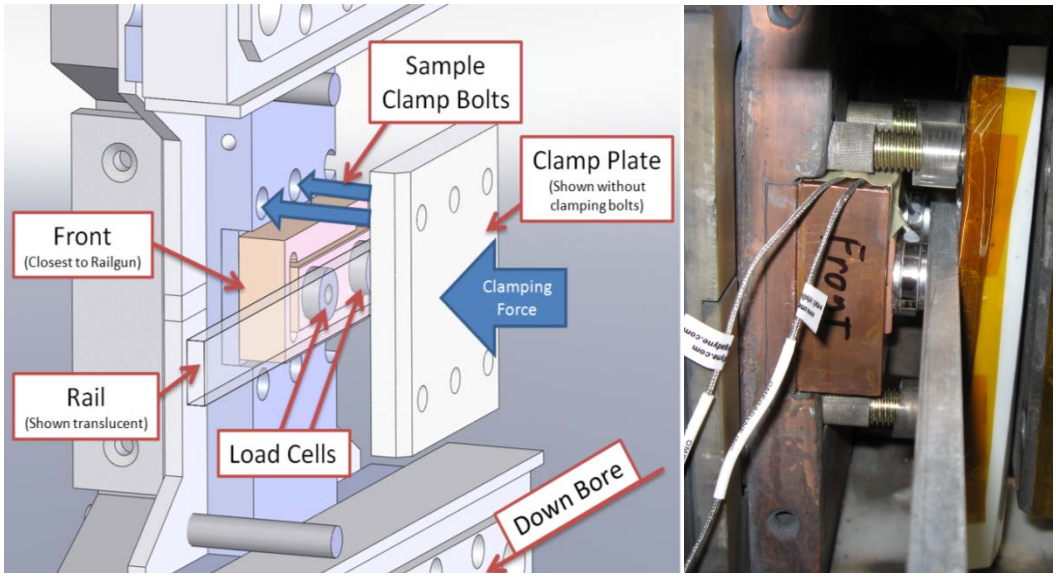

Figure 24. Schematic of the breech with load cells and the actual test setup.

To support the load cells, a copper insert was modified to accept set screws as shown on figure 25. The load cells could then be placed on the set screws, which maintained the load cell position without altering the clamping force on the load cells. The exposed set screw lengths were kept shorter than the thickness of the load cell to prevent the set screws from transferring load and altering the load cell readings. The individual load cell forces were recorded for a number of clamping bolt torque values ranging up to 150 lb-ft.

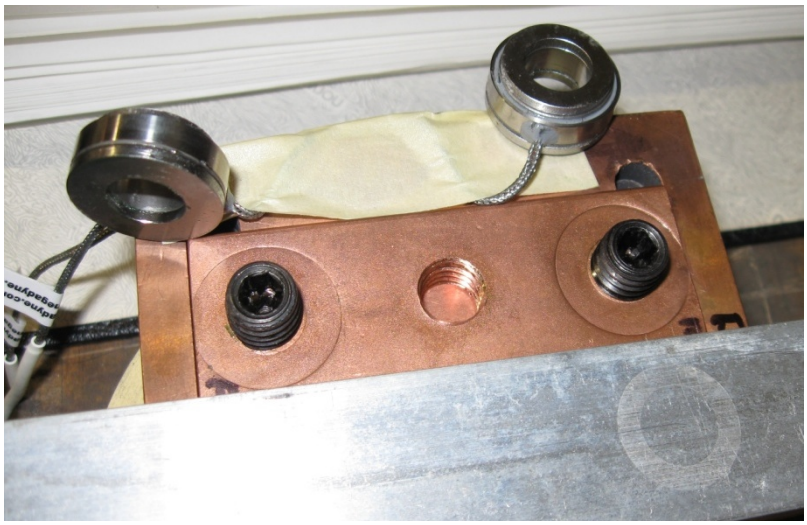

Figure 25. Measurement block with support set screws.

As expected, the force varied linearly with the applied torque (figure 26). The readings from the load cell closest to the railgun containments (labeled “front” in the figure legend) were approximately 52% lower than that of the opposite load cell, due to the shifted bolt pattern of the breech. Adding the force from the load cells yields the total clamping force on the insert and rail.

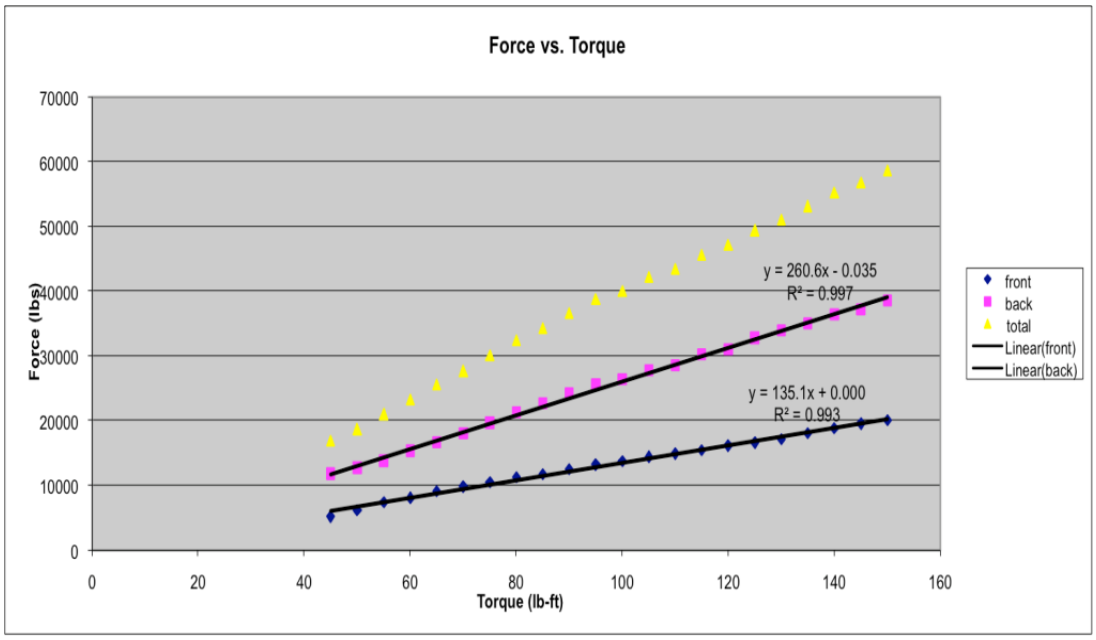

Figure 26. Force versus torque recorded from load cells data.

Considering the significant variations in load cell readings from front (towards the muzzle) to back (towards the breech), a test was conducted to check that the load cells were yielding similar readings. To verify the load cells were generating accurate readings, the two load cells were stacked in series, back to back, between the rail and the copper insert. The load cells were placed

on the center post of the insert. The insert was centered between the center set of clamping bolts where only the two center clamp bolts were tightened. Any divergence in the readings could indicate a load cell problem or calibration error. The results, as plotted in figure 27, showed good agreement between the load cell readings, which lend confidence to the measurements previously taken with the load cells in parallel. The linearity of the curves indicated consistency in the application of the clamping force.

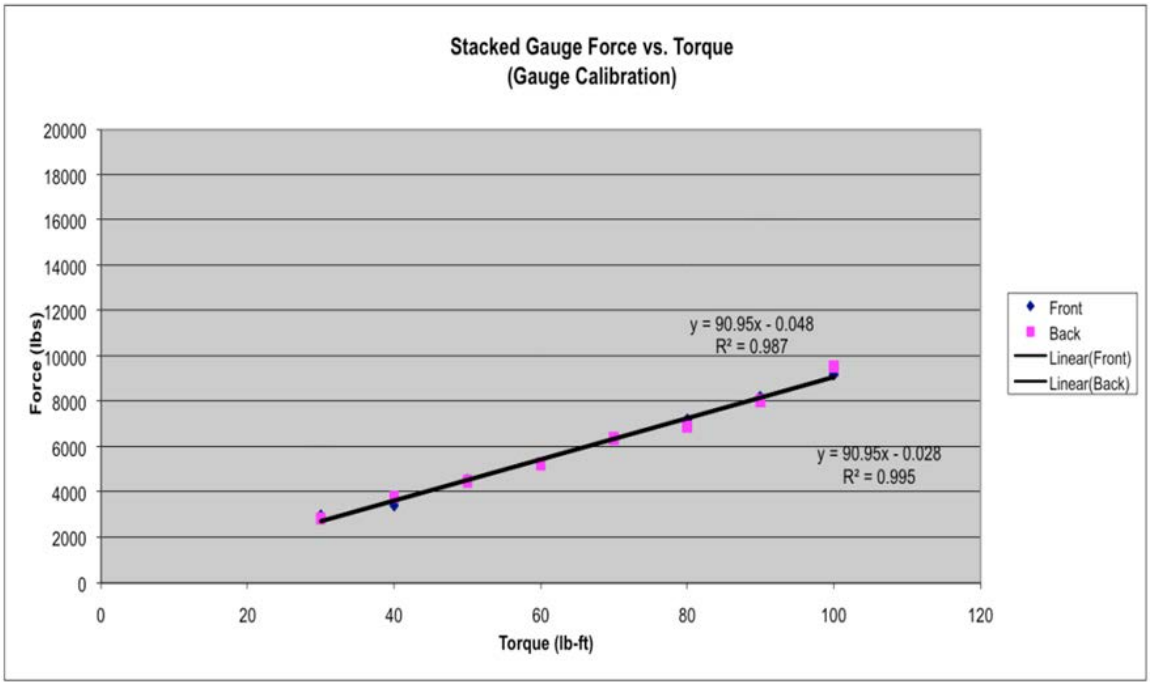

Figure 27. Stacked back to back load cells/gauge data to check calibration.

To determine if bolt wear or friction may have affected the measurement between the front and back load cells, the breech bolts were replaced. The clamping plates and bolts were taken apart, thoroughly cleaned, and lubricated. Consequently, the new measurements, as shown in figure 28, showed somewhat higher force values due to the decrease in friction.

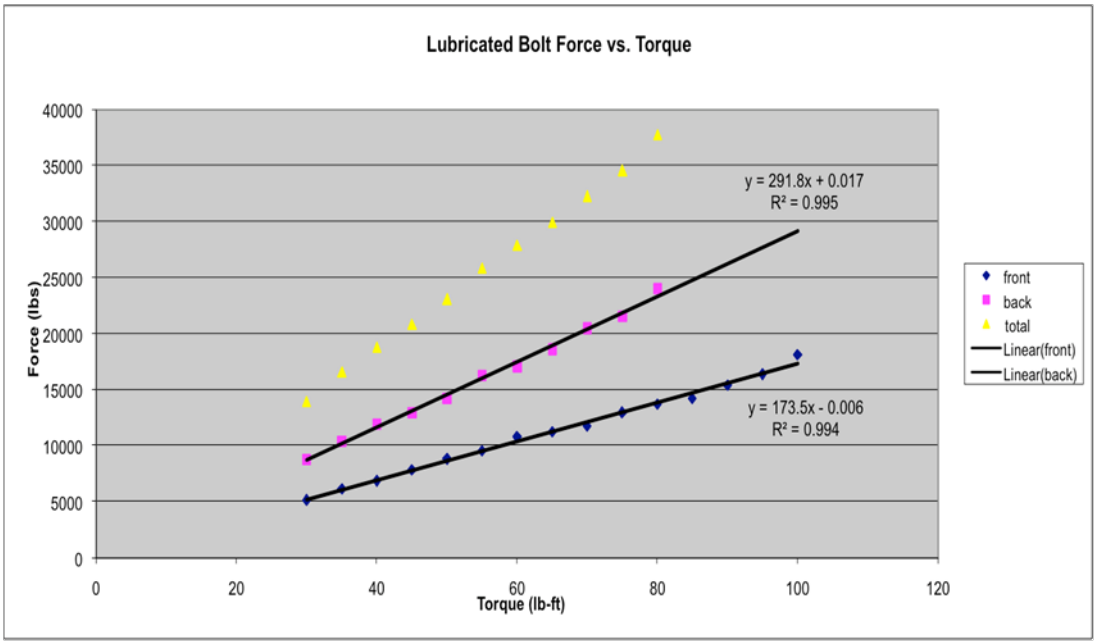

Figure 28. Measured force for lubricated bolts and threads on breech plates.

The linearity of the lines remained unchanged. The gauges, however, approached their maximum load, which prevented higher torques from being applied. The load testing showed clamping force distribution is uneven with the current breech design. In this breech design, the higher clamping force is opposite to where it is needed. Future breech designs may be able implement symmetric or even non-symmetric bolt layout to an advantage. These results also showed that without proper maintenance and lubrication of the clamping hardware, the actual clamping forces applied could be reduced (12 to 28%) from expected.

5. Breech Pressure Distribution Analysis Using Color Films

Pressure sensitive films (Pressurex^{TM}) were used to measure and record pressure distributions between the rail and inserts. A strip of film was positioned between the insert and the aluminum rail segment (figure 29), and then all six breech clamp bolts were tightened to normal firing torques (110 ft-lbs). Inserts made from aluminum 6262 and annealed copper were tested, some with pockets cut into the insert faces (figure 30).

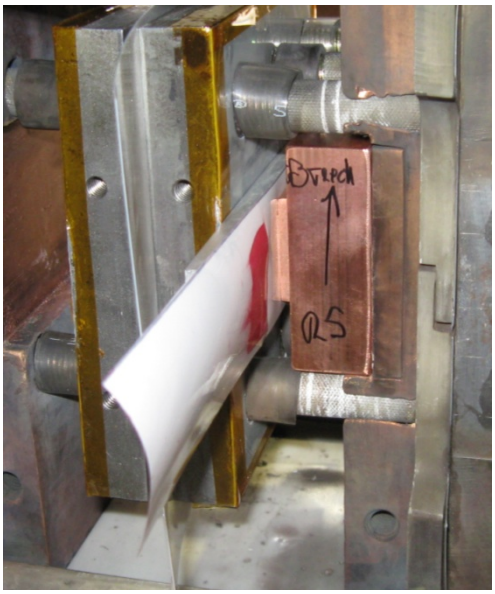

Figure 29. Pressurex™ film positioned for testing.

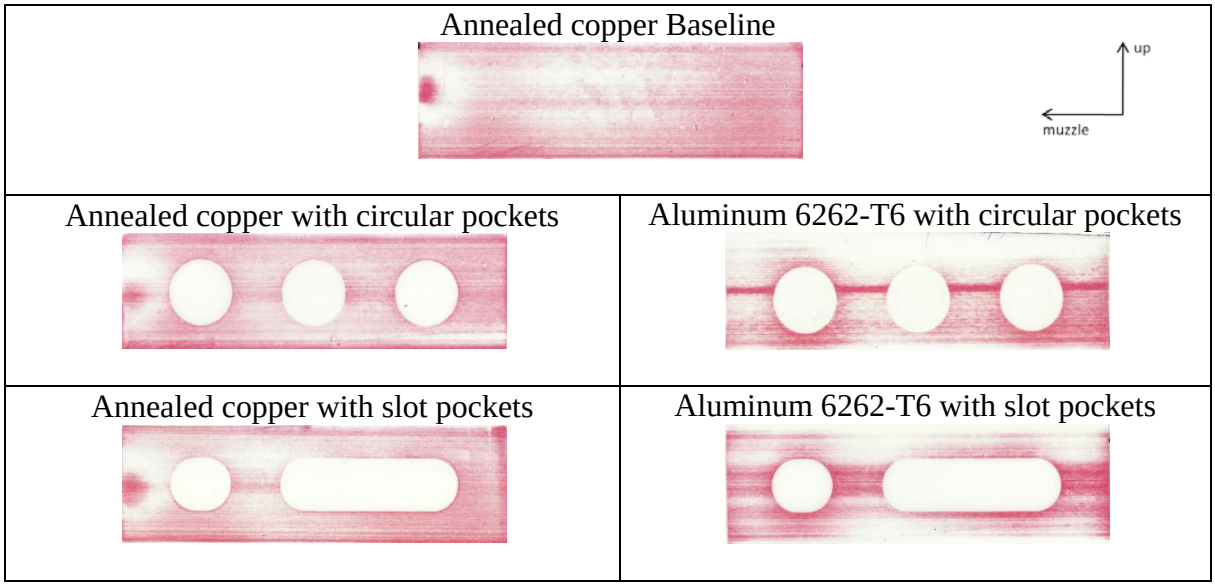

Figure 30. Inserts grouped by pocket geometry and material.

All of the film samples showed lower pressure imprints towards the muzzle compared to the trailing edge as indicated by the darker red regions produced on the film due to loading. These results further confirm the unevenness of the clamping forces measured using the load cells. Comparing the annealed copper with the aluminum inserts, the copper inserts show a more uniform pressure distribution. The aluminum inserts, however, show the majority of the pressure along the center axis while little pressure towards the edges. These results indicate the higher strength aluminum is unable to deflect enough to maintain more uniform contact pressure. It should be noted that the pressure film used has a usable range of 7,100 psi to 18,500 psi, which

means the non-pocket white areas on the imprints are likely to be carrying some load, but under minimum marking pressure of the film. With the goal to improve contact pressure uniformity, only the annealed copper inserts should be considered for future testing.

The non-uniform clamping force of the breech is also evident in the film imprints. Looking at the aluminum with circular pockets imprint, the end closest to the muzzle shows a significant amount less imprinted area than the end furthest from the gun. While the other imprints show the same trend to varying degrees, quantifying the copper imprints is hindered by a damaged breech block. The breech block shows evidence of permanent deformation caused by the load cell tests. This can be seen by the white circular regions closest to the muzzle on the films used with the copper inserts. The less ductile aluminum inserts did not flow or deflect into the cavity in the breech block, making this defect less apparent through the response of this film.

Due to the nature of the film, that only record peak loads are recorded, some areas of the film may show a greater pressure than actually exists when all bolts are tightened. To obtain more consistent results, that can be quantified, the pocket pattern tests should be repeated on a precision hydraulic press. The inserts and blocks used should also be machined true and ground flat for optimum results. In spite the suboptimal tests, the results from the force transducers and pressure sensitive film have provided useful insight into the clamping loads applied to the rail interface of ARL's railgun. In order to enhance the interface within the current system, the slot pockets have been extended to a single, near full-length pocket as can be seen in figure 31. Subsequent shots at higher current levels have shown a remarked improvement in the joint integrity. Further study is still needed to refine the contact pressure distribution.

Figure 31. Full length pocket inserts in breech blocks.

6. Conclusions and Remarks

Preliminary results show that the existing breech design could incorporate slots in the current carrying breech plates to produce a more uniform current distribution. While a thru-L shaped slot had the most effect on current distributions, further testing is necessary to optimize the number of slots, slot geometry, slot sizes and determine the dependence of optimization for these

characteristics on the applied current and energy. The information learned using the current breech surrogate could then be applied to produce a greatly improved design for a new breech.

The point of catastrophic failure for the tested “U” shorts was determined to be at 783 KA. Testing continued at less than 80% of the current or approximately 620 KA. Further testing, even with a decreased peak current limit, has not been resumed and it remains unanswered how to implement an improved interface design that would allow the loading of armatures without disconnecting the rails from the breech or opening the railgun containments during multi-shot series.

Due to the design of the existing breech, asymmetric clamping force is generated between the railgun rails and the breech. Measurements with load cells show the existing breech has almost 52% less clamping force closest to the railgun than the trailing areas due to the location of the clamping bolts. Since over one-third of the current measured is shown to be in the first one-tenth of the existing breech connection and the distribution of interface loads created by the existing hardware, catastrophic arcing is expected at higher current levels.

The results from the pressure film indicated pockets in the inserts may help produce a more uniform contact pressure between the inserts and the rails. The pressure film also indicated that the softer copper yielded a more uniform pressure distribution. The pressure imprints also showed unnoticed defects in the test hardware that could be easily corrected with more strict machining, assembly, and test setup requirements. The preliminary results from shots utilizing the slot pocket inserts, with slots that have been extended to a single, near full-length pocket, show less damage occurring to the rails and inserts than seen in previous testing.

NO. OF
COPIES ORGANIZATION

1 (PDF only) DEFENSE TECHNICAL INFORMATION CTR
DTIC OCA
8725 JOHN J KINGMAN RD
STE 0944
FORT BELVOIR VA 22060-6218

1 DIRECTOR
US ARMY RESEARCH LAB
IMNE ALC HRR
2800 POWDER MILL RD
ADELPHI MD 20783-1197

1 DIRECTOR
US ARMY RESEARCH LAB
RDRL CIO LL
2800 POWDER MILL RD
ADELPHI MD 20783-1197

1 DIRECTOR
US ARMY RESEARCH LAB
RDRL CIO MT
2800 POWDER MILL RD
ADELPHI MD 20783-1197

1 DIRECTOR
US ARMY RESEARCH LAB
RDRL D
2800 POWDER MILL RD
ADELPHI MD 20783-1197

2 IAP RSRCH INC
D BAUER
J BARBER
2763 CULVER AVE
DAYTON OH 45429-3723

1 TITAN CORPORATION
T WOLFE
4855 RUFFNER ST STE A
SAN DIEGO CA 92111

1 US ARMY RDECOM ARDEC
BENET LAB
RDAR WSB L
E KATHE
WATERVLIET ARSENAL BLDG 115
1 BUFFINGTON ST
WATERVLIET NY 12189-4000

NO. OF
COPIES ORGANIZATION

ABERDEEN PROVING GROUND

8 DIR USARL
RDRL WM
P PLOSTINS
RDRL WMM A
R EMERSON
RDRL WMM B
R KASTE
RDRL WML D
R BEYER
M DEL GÜERCIO
RDRL WML G
A MICHLIN
T BROSSEAU
RDRL WMP A
C HUMMER